Journal of Applied Fluid Mechanics, Vol. 9, No. 5, pp. 2391-2401, 2016.
Available online at www.jafmonline.net, ISSN 1735-3572, EISSN 1735-3645.
DOI: 10.18869/acadpub.jafm.68.236.25549

Free Convection Flow of a Jeffrey Fluid through a Vertical Deformable Porous Stratum

S. Sreenadh[1†], M. M. Rashidi[2, 3], K. Kumara Swamy Naidu[4] and A. Parandhama[5]

[1] *Department of Mathematics, Sri Venkateswara University, Tirupati- 517502, India*
[2] *Shanghai Key Lab of Vehicle Aerodynamics and Vehicle Thermal Management Systems, Tongji University, Address: 4800 Cao An Rd., Jiading, Shanghai 201804, China*
[3] *ENN-Tongji Clean Energy Institute of advanced studies, Shanghai, China*
[4,5] *Department of Mathematics, Sree Vidyanikethan Engineering College, Tirupati-517502,India*

†Corresponding Author Email: *drsreenadh@yahoo.co.in*

(Received August 29, 2015; accepted September 23, 2015)

ABSTRACT

Free convective flow of a Jeffrey fluid in a vertical deformable porous stratum is investigated. It is assumed that heat is generated within the fluid by both viscous and Darcy dissipations. The velocity, displacement and the temperature distributions are evaluated using a perturbation method valid for small values of buoyancy parameter N . The effects of Jeffrey parameter, ϕ_f and ϕ_s on the flow velocity and solid displacement are discussed in detail. In the absence of Jeffrey parameter, deformable porous parameters and the pressure gradient, all the results reduce to the corresponding results of Rudraiah *et al*. (1977). Higher skin friction is observed for a given buoyancy force for a non-Newtonian Jeffrey fluid when compared with Newtonian fluid. On comparing deformable and undeformable porous layers of present work and Rudraiah *et al*. (1977), we conclude that the skin friction gets reduced when the porous material is a deformable one. It is noticed that the effect of increasing Jeffrey parameter is to increase the skin friction in the deformable porous stratum.

Keywords: Jeffrey fluid; Non-newtonian fluid; Free convection; Perturbation method.

NOMENCLATURE

g	acceleration due to gravity	μ	Lame constant
K	drag coefficient	ϕ_s	volume fraction components of solid phase
K_0	thermal conductivity	ϕ_f	$1-\phi_s$, the volume fraction components of fluid phase
$\boldsymbol{p}$	pressure	λ_1	Jeffrey parameter
T	temperature	μ_f	coefficient of viscosity
T_0	ambient temperature	δ	measure of the viscous drag of the outside fluid relative to drag in the porous medium
N	buoyancy parameter	η	ratio of the bulk fluid viscosity to the apparent fluid viscosity in the porous layer
μ_a	apparent viscosity of the fluid in the porous material		
ρ	density of the fluid		
β	coefficient of linear thermal expansion of the fluid		

1. INTRODUCTION

In recent years a great deal of interest has been generated to study heat transfer in fluid flows through porous media because of their extensive applications in engineering, biology and medicine. These include heat exchange between soil and atmosphere, flow of moisture through porous industrial materials, heat exchangers with fluidized beds, fiber and granular insulation materials, packed-bed chemical reactors, oil recovery and movement of biofluid in tissue regions of blood vessels. Such tissue regions of blood vessels are being modeled as undeformable porous media (Gopalan, 1981). But it is appropriate to model them with deformable porous media. Further the influence of glycocalyx on biofluid flow within

blood vessels can be better understood with theory of flow through deformable porous media. The glycocalyx is the thin layer of glycoproteins lining the surface of endothelial cells in all blood vessels. This layer is of 1 μm thickness in capillaries and small blood vessels studied by Turner *et al*. (1983). Further this has strong influence on local flow conditions (such as wall shear stress) during the formation of atherosclerosis. In view of these facts, the study of flow through deformable porous media is necessitated.

The study of flows through deformable porous materials was initiated by Terzaghi (1925) and further developed by Biot (1941, 1955), Atkin and Craine (1976) and Kenyon (1976). This deformation theory is applied to the study of flows in biological tissue layers and articular cartilage (Jayaraman, 1983: Mow *et al*., 1984: Holmes, 1985: Oomens *et al*., 1987: and Holmes *et al*., 1990). Following the theory of mixtures given by Kenyon (1976) and Bowen (1980), Barry *et al*. (1991) modeled the porous material as a continuous binary mixture comprising of solid and fluid phases where each point in the mixture is occupied simultaneously by both fluid and solid. The solid and fluid are assumed to be intrinsically incompressible. Bulk compression of the mixture arises only by a decrease in the fluid fraction. The deformation is small and hence the intrinsic properties of the porous medium are taken as constant. Based on this, he derived the governing equations for the flow in deformable porous media and investigated the flow of a Newtonian fluid over a thin deformable porous layer. Farina *et al*. (1997) described the application of a deformable porous media model to the manufacturing of composite materials by compression moulding. Ambrosi (2002) is studied infiltration through deformable porous media. Wen *et al*. (2009) investigated dynamic responses of a viscous fluid flow introduced under a time dependent pressure gradient in a rigid cylindrical tube that is lined with a deformable porous surface layer. Sreenadh *et al*. (2014) discussed Couette flow over a deformable permeable bed.

Flow with porous medium is a topic of prime importance now-a-days owing to its applications in metal production, underground bed flow and oil recovery from partially depleted reservoirs. Flows through undeformable porous media have been studied very well by several researchers using classical Darcy or modified Darcy laws (Muskat, 1937 and Tam, 1969). Bear (1972) was the first to present and use the continuum approach in modeling flow and transport phenomena. Rudraiah and Nagaraj (1977) made a study on natural convection through a vertical porous stratum including both viscous and Darcy resistances. It is observed that permeability acts to decrease the dissipation effects. Umavathi and Malashetty (1999) discussed the Oberbeck convection flow of a couple stress fluid through a vertical porous stratum. MHD free convection adjacent to a vertical surface with Ohmic heating and viscous dissipation is investigated by Chen (2004). Unsteady boundary layer flow of a viscous, electrically conducting and heat absorbing fluid along a semi-infinite vertical permeable moving plate has been studied by Chamka (2004). Ebaid *et al*. (2006) have analysed the peristaltic transport of a Newtonian fluid in an asymmetric channel through a porous medium. Zaheer Abbas and Tasawar Hayat (2008) studied the radiation effects on the magnetohydrodynamic flow of an incompressible viscous fluid in a porous space using homotopy analysis method. Srinivas *et al*. (2011) discussed the effect of chemical reaction on space porosity on MHD peristaltic flow in a vertical asymmetric channel. Shadloo and Kimiaeifar (2011) obtained an analytical solution for magnetohydrodynamic flows of viscoelastic fluids in converging/diverging channels applying homotopy perturbation method. Rashidi *et al*. (2012) analysed MHD convective flow due to a rotating disk with viscous dissipation and Ohmic heating. Natural convection flow of a third grade fluid between two parallel plates is studied by Rashidi *et al*. (2013a) applying multi-step differential transform method. Rashidi *et al*. (2013b) studied entropy generation in steady MHD flow due to a rotating porous disk in a nanofluid employing Von Karman transformation. Rashidi *et al*. (2014a) examined MHD fluid flow over a permeable vertical stretching sheet with radiation and buoyancy effects. Lie group solution for free convective flow of a nanofluid past a chemically reacting horizontal plate in porous media has been studied by Rashidi *et al*. (2014b). Rashidi and Freidoonimehr (2014) investigated entropy generation in magnetohydrodynamic stagnation-point flow with heat transfer in a porous medium via DTM- Pade. Abolbashari *et al*. (2014) presented the entropy analysis in an unsteady magneto-hydrodynamic nanofluid regime adjacent to an accelerating stretching permeable surface. Rashidi *et al*. (2015) presented entropy generation analysis for stagnation point flow through a porous medium over a permeable stretching surface. Prasad *et al*. (2015) studied the effects of temperature-dependent transport properties on MHD convection flow in a vertical channel. Freidoonimehr *et al*. (2015) obtained dual solutions for the problem of magneto-hydrodynamic Jeffery–Hamel nanofluid flow in non-parallel walls employing a new analytical technique, Predictor Homotopy Analysis Method (PHAM).

The behavior of some of the biofluids like blood, synovial fluid etc., demand the use of non-Newtonian models. Now-a-days Jeffrey model is attracting the attention of researchers to describe many biological situations. Vajravelu *et al*. (2011) discussed the convective peristaltic flow of a Jeffrey fluid in a vertical porous stratum. Tariq Javed *et al*. (2013) analysed the boundary layer flow of a non-Newtonian fluid over a stretching sheet using Keller box method. Sreenadh *et al*. (2013) obtained a solution for free convective MHD Jeffrey fluid flow between two coaxial permeable cylinders assuming quadratic density temperature variation. Noreen Sher Akbar *et al*. (2013) analyzed characteristics of Jeffrey fluid model for peristaltic flow of chyme in

small intestine with magnetic field. Abd-Alla *et al*. (2014) have investigated the peristaltic flow of a Jeffrey fluid in an asymmetric channel. Santhosh Nallapu and Radhakrishnamacharya (2014) studied Jeffrey fluid flow in the presence of magnetic field through porous medium in tubes of small diameters. Available literature on non-Newtonian models shows that not much attention has been given in the non-Newtonian fluid flow in a vertical deformable porous stratum.

In view of this the authors envisage to study natural convection flow of a non-Newtonian Jeffrey fluid in a deformable vertical porous layer. Here Jeffrey model is chosen as it is one of the simplest models for non-Newtonian fluids and this model reduces to Newtonian model as a special case by taking $\lambda_1 \to 0$. The velocity, displacement and temperature are obtained. The impact of buoyancy on the flow pattern is discussed in detail.

2. MATHEMATICAL FORMULATION

Consider the steady fully developed, free convective flow of a Jeffrey fluid through a vertical deformable porous stratum as shown in Fig.1. The porous material is modeled as a continuous binary mixture of solid and fluid phases where each point in the mixture is occupied continuously by both fluid and solid (Barry et. al, 1991). x -axis is taken midway in the channel and y -axis perpendicular to it. The deformations are assumed to be small and are predominantly in the-direction. It is assumed that heat is generated within the fluid by both viscous and Darcy dissipations. The walls are placed at a distance $2b$ and maintained at a constant temperature T_1 . The fluid velocity and solid displacement in the deformable layer are assumed to be $(v,0,0)$ and $(u,0,0)$, respectively. A pressure gradient $\frac{\partial p}{\partial x}$ is applied, producing an axially directed flow. Due to the assumptions of an infinite channel there will be no x dependence in any of the terms except the pressure. For simplicity we restrict our discussion to the half width of the channel.

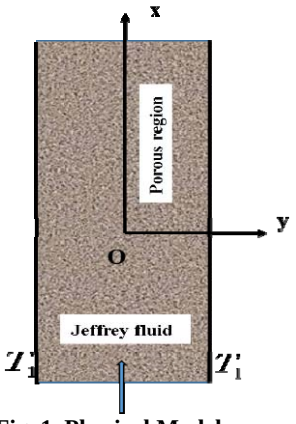

Fig. 1. Physical Model.

With the assumptions mentioned above, for the fully developed flow model under consideration, the basic equations of the problem for deformable porous region reduce to (Barry, 1991, Rudraiah *et al*., 1977).

$$\frac{2\mu_a}{1+\lambda_1}\frac{\partial^2 v}{\partial y^2} - \phi_f \frac{\partial p}{\partial x} - Kv + \rho g \beta (\mathrm{T} - \mathrm{T}_0) = 0 \qquad (1)$$

$$\mu \frac{\partial^2 u}{\partial y^2} - \phi_s \frac{\partial p}{\partial x} + Kv = 0 \qquad (2)$$

$$\frac{\partial^2 T}{\partial y^2} + \frac{2\mu_a}{K_0(1+\lambda_1)}\left(\frac{\partial v}{\partial y}\right)^2 + \frac{K}{K_0}v^2 = 0 \qquad (3)$$

The boundary conditions are

$$u = 0, v = 0, T = T_1 \quad \text{at} \quad y = b \qquad (4)$$

$$\frac{du}{dy} = 0, \frac{dv}{dy} = 0, \frac{dT}{dy} = 0 \quad \text{at} \quad y = 0$$

3. NON-DIMENSIONALIZATION OF THE FLOW QUANTITIES

It is convenient to introduce the following non-dimensional quantities.

$$y^* = \frac{y}{b}, x^* = \frac{x}{b}, v^* = \frac{2\mu_a v}{\rho g \beta b^2 (T_1 - T_0)},$$
$$u^* = \frac{\mu u}{\rho g \beta b^2 (T_1 - T_0)},$$
$$\theta = \frac{T - T_0}{T_1 - T_0}, p^* = \frac{p}{\rho g \beta b (T_1 - T_0)} \qquad (5)$$

In view of the above dimensionless quantities, the Eqs. (1) – (4) take the following form. The asterisks $(*)$ are neglected here after.

$$\frac{1}{1+\lambda_1}\frac{d^2 v}{dy^2} - \phi_f \frac{dp}{dx} - \delta\eta v + \theta = 0 \qquad (6)$$

$$\frac{d^2 u}{dy^2} - \phi_s \frac{dp}{dx} + \delta\eta v = 0 \qquad (7)$$

$$\frac{d^2\theta}{dy^2} + \frac{N}{1+\lambda_1}\left(\frac{dv}{dy}\right)^2 + N\,\delta\eta v^2 = 0 \qquad (8)$$

Where

$$\delta = \frac{Kb^2}{\mu_f}, \eta = \frac{\mu_f}{2\mu_a}, N = \frac{\rho_0 g^2 \beta^2 b^4 (T_1 - T_0)}{K_0(2\mu_a)}.$$

The boundary conditions are

$$u = 0, v = 0, \theta = 1 \quad \text{at} \quad y = 1$$

$$\frac{du}{dy} = 0, \frac{dv}{dy} = 0, \frac{d\theta}{dy} = 0 \quad \text{at} \quad y = 0 \qquad (9)$$

4. SOLUTION OF THE PROBLEM

The governing momentum and energy Eqs. (6) to (9) are coupled partial differential equations that cannot be solved in closed form. In most of the practical problems perturbation technique is used to solve these types of non-linear equations. We can write

$$(u, v, \theta, p) = (u_0, v_0, \theta_0, p_0) + N\,(u_1, v_1, \theta_1, p_1) + \ldots\ldots \tag{10}$$

Using the above relation in Eqs. (6)-(9), we obtain a system of equations of different orders.

4.1. System of Order N^0

The governing equations of the zeroth- order are

$$\frac{1}{1+\lambda_1}\frac{d^2 v_0}{dy^2} - \phi_f \frac{dp_0}{dx} - \delta\eta v_0 + \theta_0 = 0 \tag{11}$$

$$\frac{d^2 u_0}{dy^2} - \phi_s \frac{dp_0}{dx} + \delta\eta v_0 = 0 \tag{12}$$

$$\frac{d^2 \theta_0}{dy^2} = 0 \tag{13}$$

The appropriate boundary conditions are

$$u_0 = 0, v_0 = 0, \theta_0 = 1 \quad \text{at} \quad y = 1 \tag{14}$$

$$\frac{du_0}{dy} = 0, \frac{dv_0}{dy}, \frac{d\theta_0}{dy} = 0 \quad \text{at} \quad y = 0$$

Solving the Eqs. (11)-(13) with the use of boundary conditions (14) and we obtain the zeroth-order fluid velocity, solid displacement and the fluid temperature as

$$v_0 = 2B_1 \cosh a_1\sqrt{1+\lambda_1}\, y + a_2 \tag{15}$$

$$u_0 = C_1 + a_{14} y^2 - \frac{2B_1 \cosh a_1\sqrt{1+\lambda_1}\, y}{1+\lambda_1} \tag{16}$$

$$\theta_0 = 1 \tag{17}$$

We note that expression for zeroth order velocity reduces to the corresponding results of Rudraiah *et al*. (1977) for the natural convection flow of a Newtonian fluid through a vertical undeformable porous stratum by taking $\lambda_1 = 0, \phi_f = 0, \delta\eta = \sigma^2$.

4.2. System of Order N^1

The governing equations of the first- order are

$$\frac{1}{1+\lambda_1}\frac{d^2 v_1}{dy^2} - \phi_f \frac{dp_1}{dx} - \delta\eta v_1 + \theta_1 = 0 \tag{18}$$

$$\frac{d^2 u_1}{dy^2} - \phi_s \frac{dp_1}{dx} + \delta\eta v_1 = 0 \tag{19}$$

$$\frac{d^2 \theta_1}{dy^2} + \frac{1}{1+\lambda_1}\left(\frac{dv_0}{dy}\right)^2 + \delta\eta v_0^2 = 0 \tag{20}$$

The appropriate boundary conditions are

$$u_1 = 0, v_1 = 0, \theta_1 = 0 \quad \text{at} \quad y = 1$$

$$\frac{du_1}{dy} = 0, \frac{dv_1}{dy} = 0, \frac{d\theta_1}{dy} = 0 \text{ at} \quad y = 0 \tag{21}$$

Solving the Eqs. (18)-(20) with the use of boundary conditions (21), we obtain the first-order fluid velocity, solid displacement and fluid temperature as

$$\begin{aligned} v_1 = {} & 2B_3 \cosh a_1\sqrt{1+\lambda_1}\, y + a_4 - a_5 y^2 \\ & + a_6 \cosh 2a_1\sqrt{1+\lambda_1}\, y + a_7 y \sinh a_1\sqrt{1+\lambda_1}\, y \end{aligned} \tag{22}$$

$$\begin{aligned} u_1 = {} & a_{15} + a_9 y^2 + a_{10} y^4 + a_{11}\frac{\cosh a_1\sqrt{1+\lambda_1}\, y}{1+\lambda_1} - \\ & a_{12} \cosh 2a_1\sqrt{1+\lambda_1}\, y - a_7 \frac{y \sinh a_1\sqrt{1+\lambda_1}\, y}{1+\lambda_1} \end{aligned} \tag{23}$$

$$\begin{aligned} \theta_1 = {} & a_3 - \frac{B_1^2 \cosh 2a_1\sqrt{1+\lambda_1}\, y}{1+\lambda_1} - \frac{a_1^2 a_2^2}{2} y^2 - \\ & 4a_2 \frac{B_1 \cosh a_1\sqrt{1+\lambda_1}\, y}{1+\lambda_1} \end{aligned} \tag{24}$$

The expression for the velocity is given by

$$v = v_0 + N v_1, \tag{25}$$

where v_0 and v_1 are given by the Eqs. (15) and (22). The expression for the displacement is

$$u = u_0 + N u_1, \tag{26}$$

where u_0 and u_1 are given by the Eqs. (16) and (23). The expression for the temperature is given by

$$\theta = \theta_0 + N\theta_1, \tag{27}$$

where θ_0 and θ_1 are given by the Eqs. (17) and (24).

5. SKIN FRICTION

Knowing the velocity field we can now calculate the skin friction, which is given by

$$\begin{aligned} |\tau| = \left(\frac{dv}{dy}\right)_{y=1} = {} & 2a_1 B_1 \sqrt{1+\lambda_1} \sinh a_1\sqrt{1+\lambda_1} \\ & + \mathrm{N}\begin{bmatrix} 2a_1 B_3 \sqrt{1+\lambda_1} \sinh a_1\sqrt{1+\lambda_1}\, \mathrm{y} - 2a_5 y \\ + 2a_1 a_6 \sqrt{1+\lambda_1} \sinh 2a_1\sqrt{1+\lambda_1}\, \mathrm{y} \\ + a_7 (\mathrm{y} a_1\sqrt{1+\lambda_1} \cosh a_1\sqrt{1+\lambda_1}\, \mathrm{y} \\ + \sinh a_1\sqrt{1+\lambda_1}\, \mathrm{y}) \end{bmatrix} \end{aligned} \tag{28}$$

6. RATE OF HEAT TRANSFER

The rate of heat transfer at the wall $y = 1$ is given by

$$Nu = -\left(\frac{\partial\theta}{\partial y}\right)_{y=1} = -N\left(\begin{array}{l}\dfrac{-2a_1B_1^{\,2}\sqrt{1+\lambda_1}\sinh 2a_1\sqrt{1+\lambda_1}}{(1+\lambda_1)} - \\ a_1^2a_2^2 - \dfrac{4a_1a_2B\sqrt{1+\lambda_1}\sinh a_1\sqrt{1+\lambda_{1_1}}}{(1+\lambda_1)}\end{array}\right) \quad (29)$$

7. RESULTS AND DISCUSSIONS

The solutions for coupled equations for the fluid velocity (v), displacement (u) and temperature (θ) are evaluated numerically for different values of physical parameters such as Jeffrey parameter λ_1, the pressure gradient G, the viscous parameter ϕ_f, the viscous drag parameter δ and the parameter η is the ratio of the bulk fluid viscosity to the apparent fluid viscosity in the porous layer which are depicted in Figs. 2 to 25.

The variation of temperature θ with y is calculated from Eq. (27) for different values of $\delta,\eta,\phi_f,\phi_s,G,N,\lambda_1$ and is shown in Figs. 2 to 8. We observe that the temperature θ decreases with the increase in δ,η,ϕ_f,G, but it exhibits opposite behavior with the increase in ϕ_s,N,λ_1.

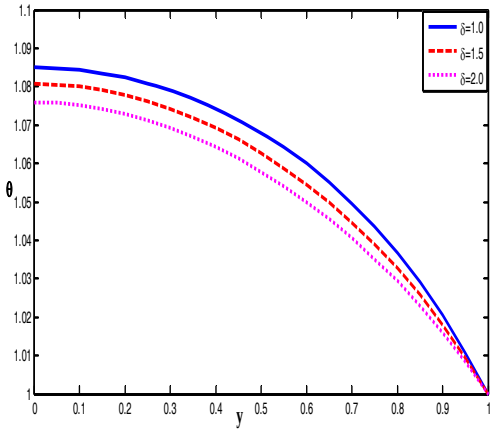

Fig. 2. The temperature profile θ for different values of δ for fixed

$\eta=1,\phi_f=0.5,\phi_s=0.5,G=0.1,\ N=1,\lambda_1=0.1$.

The variation of velocity profile v with y is calculated from Eq. (25) for different values of $\delta,\eta,\phi_f,\phi_s,G,N,\lambda_1$ and is shown in Figs. 9 to 15. Here we observe that the velocity V decreases with the increase in δ,η,ϕ_f,G whereas it increases with the increase in ϕ_s,N,λ_1.

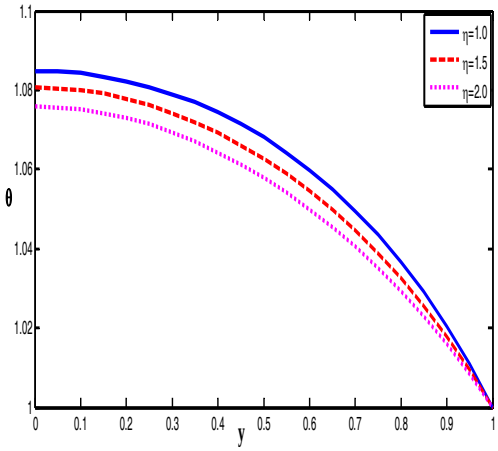

Fig. 3. The temperature profile θ for different values of η for fixed

$\delta=1,\phi_f=0.5,\phi_s=0.5,G=0.1,\ N=1,\lambda_1=0.1$.

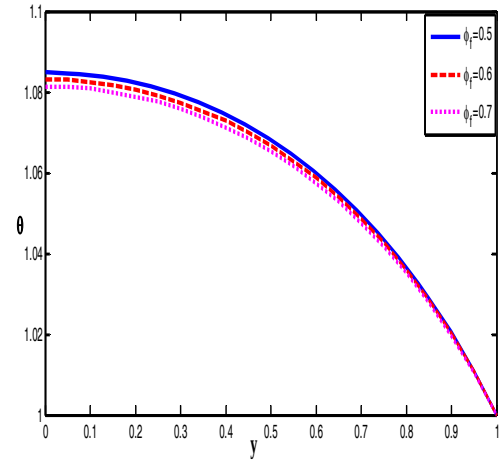

Fig. 4. The temperature profile θ for different values of ϕ_f for fixed

$\eta=1,\delta=1,\phi_s=0.5,G=0.1,\ N=1,\lambda_1=0.1$.

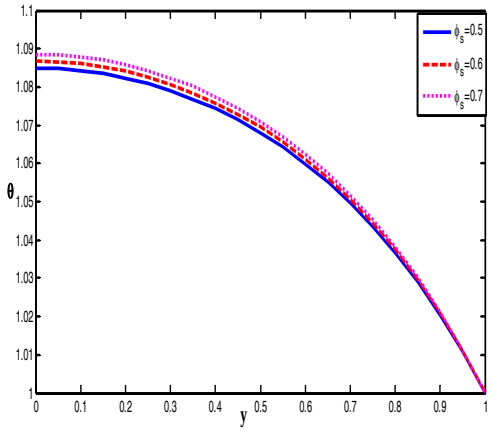

Fig. 5. The temperature profile θ for different values of ϕ_s for fixed

$\eta=1,\phi_f=0.5,\delta=1,G=0.1,\ N=1,\lambda_1=0.1$.

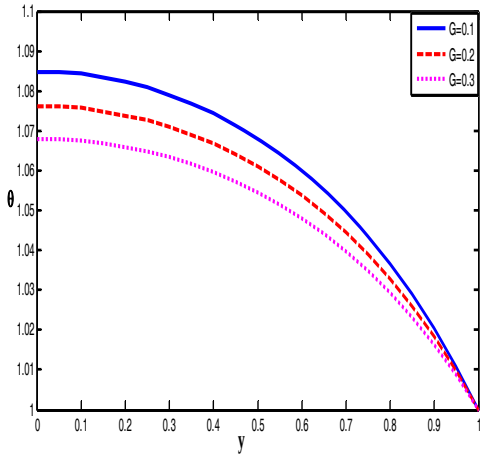

Fig. 6. The temperature profile θ for different values of G for fixed

$\eta=1,\phi_f=0.5,\phi_s=0.5,\delta=1,\ N=1,\lambda_1=0.1$.

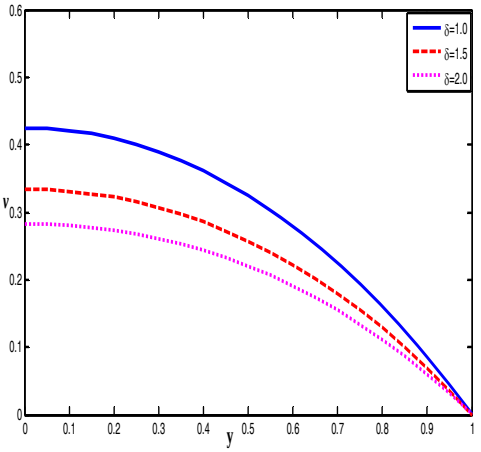

Fig. 9. The Velocity profile v for different values of δ for fixed

$\eta=1,\phi_f=0.5,\phi_s=0.5,\ G=0.1,\ N=1,\lambda_1=0.1$.

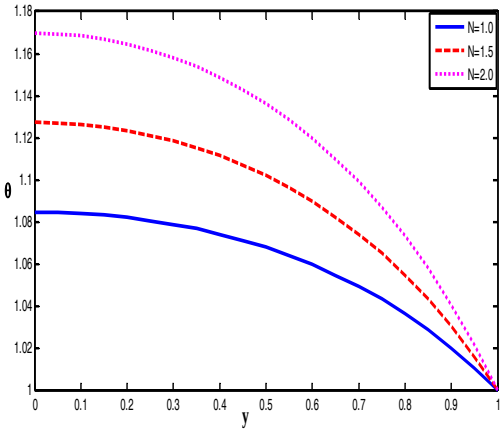

Fig. 7. The temperature profile θ for different values of N for

$\eta=1,\phi_f=0.5,\phi_s=0.5,\delta=1,\ G=1,\lambda_1=0.1$.

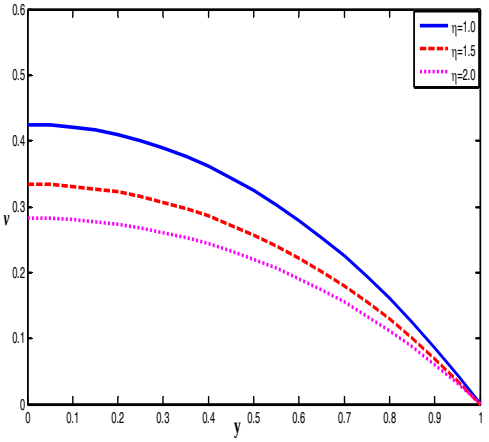

Fig. 10. The Velocity profile v for different values of η for fixed

$\delta=1,\phi_f=0.5,\phi_s=0.5,G=0.1,\ N=1,\lambda_1=0.1$.

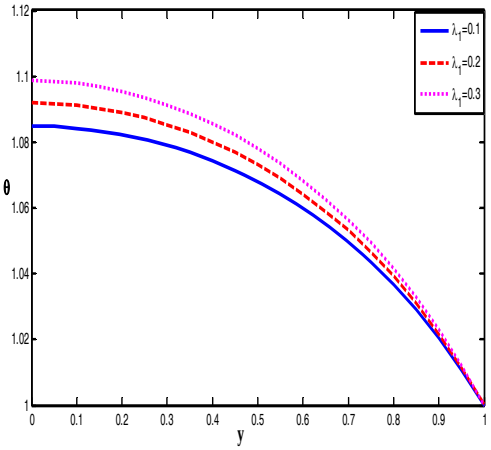

Fig. 8. The temperature profile θ for different values of λ_1 for fixed

$\eta=1,\phi_f=0.5,\phi_s=0.5,G=0.1,\ N=1,\delta=1$.

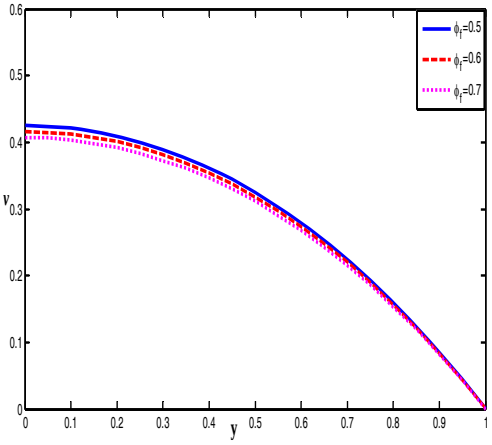

Fig. 11. The Velocity profile v for different values of ϕ_f for fixed

$\eta=1,\delta=1,\phi_s=0.5,G=0.1,\ N=1,\lambda_1=0.1$.

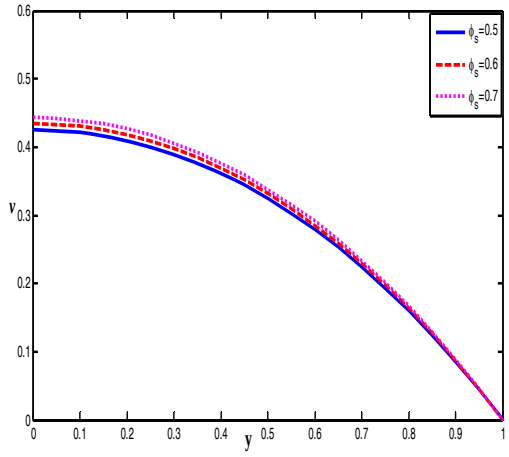

Fig. 12. The Velocity profile v for different values of ϕ_s for fixed

$\eta = 1, \phi_f = 0.5, \delta = 1, G = 0.1, N = 1, \lambda_1 = 0.1$.

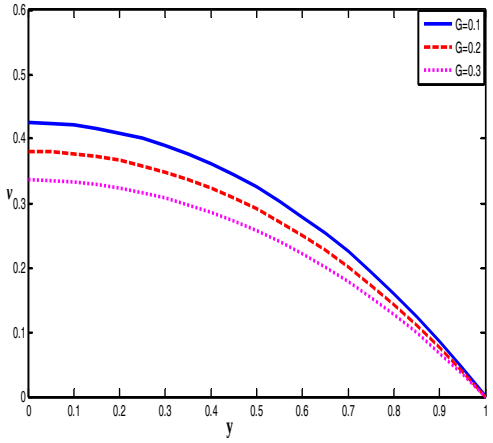

Fig. 13. The Velocity profile v for different values of G for fixed

$\eta = 1, \phi_f = 0.5, \phi_s = 0.5, \delta = 1, N = 1, \lambda_1 = 0.1$.

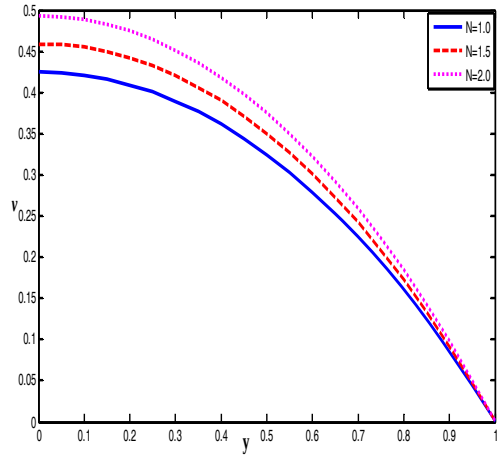

Fig. 14. The Velocity profile v for different values of N for fixed

$\eta = 1, \phi_f = 0.5, \phi_s = 0.5, G = 0.1, \delta = 1, \lambda_1 = 0.1$.

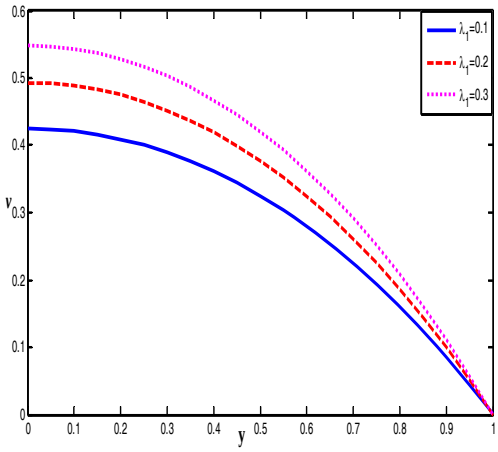

Fig. 15. The Velocity profile v for different values of λ_1 for fixed

$\eta = 1, \phi_f = 0.5, \phi_s = 0.5, G = 0.1, N = 1, \delta = 1$.

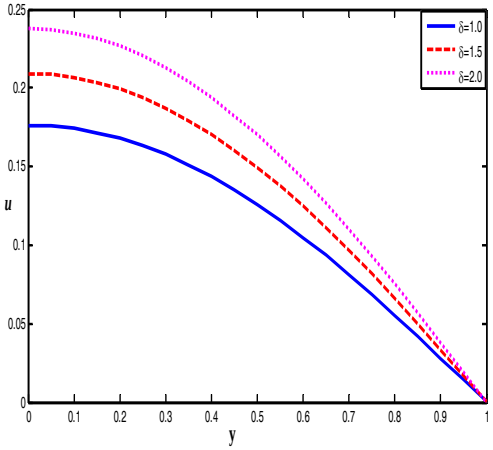

Fig. 16. The displacement profile u for different values of δ for fixed

$\eta = 1, \phi_f = 0.5, \phi_s = 0.5, G = 0.1, N = 1, \lambda_1 = 0.1$.

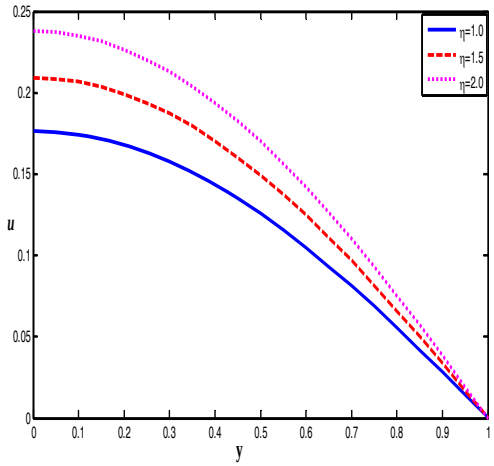

Fig. 17. The displacement profile u for different values of η for fixed

$\delta = 1, \phi_f = 0.5, \phi_s = 0.5, G = 0.1, N = 1, \lambda_1 = 0.1$.

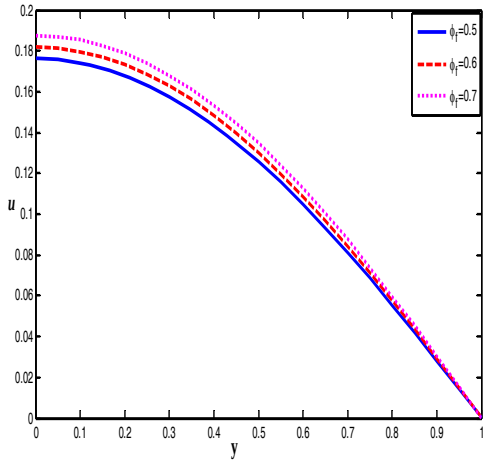

Fig. 18. The displacement profile u for different values of ϕ_f for fixed

$\delta = 1, \eta = 1, \phi_s = 0.5, G = 0.1,\ N = 1, \lambda_1 = 0.1$.

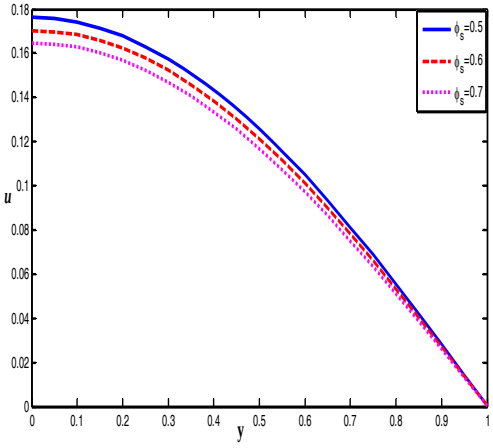

Fig. 19. The displacement profile u for different values of ϕ_s for

$\delta = 1, \phi_f = 0.5, \eta = 1, G = 0.1,\ N = 1, \lambda_1 = 0.1$.

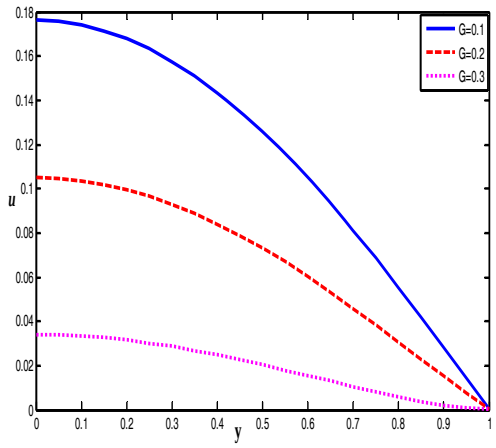

Fig. 20. The displacement profile u for different values of G for

fixed $\delta = 1, \phi_f = 0.5, \phi_s = 0.5, \eta = 1,\ N = 1, \lambda_1 = 0.1$.

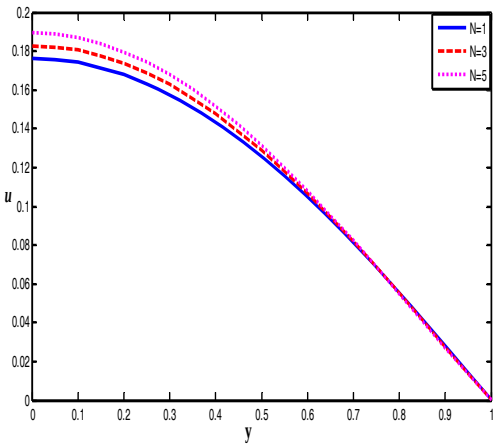

Fig. 21. The displacement profile u for different values of N for fixed

$\delta = 1, \phi_f = 0.5, \phi_s = 0.5, G = 0.1,\ \eta = 1, \lambda_1 = 0.1$.

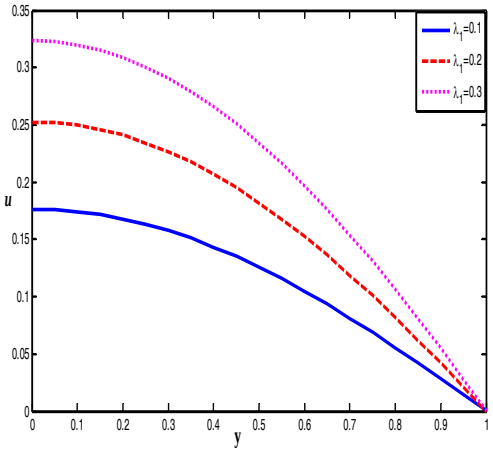

Fig. 22. The displacement profile u for different values of λ_1 for fixed

$\eta = 1, \phi_f = 0.5, \phi_s = 0.5, G = 0.1,\ N = 1, \delta = 1$.

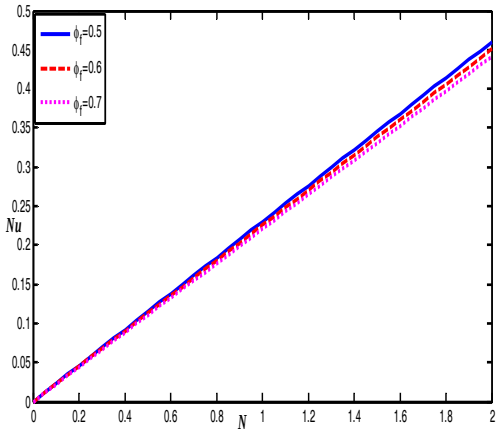

Fig. 23. The Nusselt number Nu for different values of ϕ_f for fixed

$\eta = 1,\ \phi_s = 0.5, G = 0.1, \delta = 1, \lambda_1 = 0.1$.

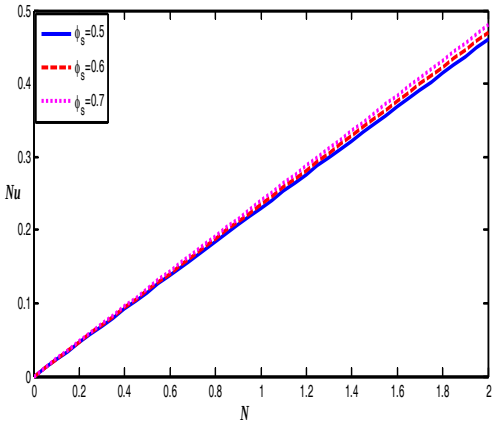

Fig. 24. The Nusselt number Nu for different values of ϕ_s for fixed

$$\eta = 1,\ \phi_f = 0.5, G = 0.1, \delta = 1, \lambda_1 = 0.1.$$

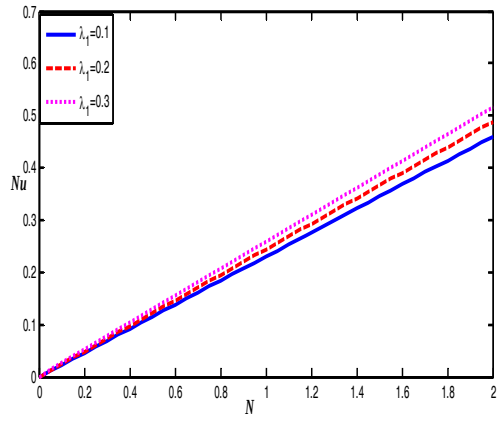

Fig. 25. The Nusselt number Nu for different values of λ_1 for fixed

$$\eta = 1,\ \phi_s = 0.5, G = 0.1, \delta = 1, \phi_f = 0.5.$$

The variation of displacement profile u with y is calculated from Eq. (26) for different values of $\delta, \eta, \phi_f, \phi_s, G, N, \lambda_1$ and is shown in Figs. 16 to 22. Here we observe that the displacement u increases with the increase in $\lambda_1, \delta, \eta, \phi_f$ and N but it exhibits opposite behavior with the increase in ϕ_s, G.

The magnitude of the skin friction is numerically evaluated from Eq. (28) for different values of buoyancy parameter N and is presented in Table 1. It is found that the skin friction at the vertical wall $y = 1$ increases with increasing buoyancy parameter N. The same behavior is noticed in the case of vertical undeformable porous layer (Rudraiah *et al*., 1977). The skin friction at the wall $y = 1$ increases with the increasing buoyancy parameter N. Higher skin friction is observed for a given buoyancy force for a non-Newtonian Jeffrey fluid when compared with Newtonian fluid.

The magnitude of the Skin friction values for various values of Jeffrey parameter λ_1 are calculated from Eq. (28) and presented in Table 2. It is found that the effect of increasing Jeffrey parameter is to increase the skin friction in the deformable porous stratum.

The rate of heat transfer at $y = 1$ is evaluated from Eq. (29) for different values of $\phi_f, \phi_s, \lambda_1$ and is shown in Figs. 23 to 25. Here we observe that the Nusselt number decreases with the increase in ϕ_f and increases with the increase in ϕ_s and Jeffrey parameter λ_1.

Table 1 Skin friction τ at $y = 1$ for different values of N

S.No		$N = 1$	$N = 2$	$N = 3$
1	Rudraiah *et al* (1977) (undeformable porous layer)	0.8056	0.8497	0.8937
2	Present work (deformable porous layer with $\lambda_1 = 0$)	0.7252	0.7268	0.7285
3	Present work (with $\lambda_1 = 0$)	1.0660	1.3006	1.5352

Table 2 Skin friction τ at $y = 1$ for different values of λ_1

λ_1	0	0.2	0.4	0.6	0.8	1.0
τ	0.7252	1.0660	1.3017	1.4741	1.6059	1.7103

ACKNOWLEDGEMENT

One of the authors Prof S. Sreenadh would like to thank UGC for providing financial support through the major research project. F.No.41-778/2012 (SR) to undertake this work.

REFERENCES

Abd-Alla, A. M., S. M. Abo-Dahab and M. M. Albalawi (2014). Magnetic field and gravity effects on Peristaltic transport of a Jeffrey fluid in an asymmetric channel, *Abstract and Applied Analysis*, 11.

Abolbashari, M. H., F. Nazari Freidoonimehr and

M. M. Rashidi (2014). Entropy analysis for an unsteady MHD flow past a stretching permeable surface in nano-fluid. *Powder Technology* 267, 256–267.

Ambrosi, D. (2002). Infiltration through Deformable Porous Media. *Z. Angew. Math. Mech.* 82(2), 115-124.

Atkin, R. J. and R. E. Craine (1976). Continuum theories of mixtures: Basic theory and historical development. *Quart. J. Mech. Appl Math*. 29, 209-244.

Barry, S. I., K. H. Parker and G. K. Aldis (1991). Fluid flow over a thin deformable porous layer. *Z. Angewandte Math. Phys.* 42, 633–648.

Bear, J. (1972). Dynamics of Fluids in Porous Media, Dover, New York.

Biot, M. A. (1941). General theory of three-dimensional consolidation. *J. Appl. Phys.* 12,155-164.

Biot, M. A. (1955). Theory of elasticity and consolidation for a porous anisotropic solid. *J. Appl. Phys.* 26, 182-185.

Chamkha, A. J. (2004). Unsteady MHD convective heat and mass transfer past a semi-infinite vertical permeable moving plate with heat absorption. Int. J. Engng. Sci. 42, 217–230.

Chen, C. H. (2004). Combined heat and mass transfer in MHD free convection from a vertical surface with Ohmic heating and viscous dissipation. *Int. J. Eng. Sci.* 42, 699-713.

Ebaid, A. (2008). Effects of magnetic field and wall slip conditions on the peristaltic transport of a Newtonian fluid in an asymmetric channel. *Physics Letters A* 372(24), 4493–4499.

Farina, A., P. Cocito and G. Boretto (1997). Flow in Deformable Porous Media: Modelling and Simulations of Compression Moulding Processes. *Mathl. Comput. Modelling.* 2(11), l-15.

Freidoonimehr, N. and M. M. Rashidi (2015). Dual Solutions for MHD Jeffery–Hamel Nano-fluid Flow in Non-parallel Walls using Predictor Homotopy Analysis Method. *Journal of Applied Fluid Mechanics.* 8(4), 911-919.

Gopalan, N. P. (1981). Pulsatile blood flow in a rigid pulmonary alveolar sheet with porous walls. *Bulletin of Mathematical Biology*. 43(5), 563-577.

Holmes, M. H. (1985). A theoretical analysis for determining the nonlinear hydraulic permeability of a soft tissue from a permeation experiment. *Bull. Math. Biology.* 47, 669-683.

Holmes, M. H. and V. C. Mow (1990). The nonlinear characteristics of soft gels and hydrated connective tissues in ultrafiltration. *J. Biomechanics*. 23, 1145-1156.

Javed, T., N. Ali, Z. Abbas and M. Sajid (2013). Flow of an Eyring-Powell Non-Newtonian Fluid over a Stretching Sheet. *Chem. Eng. Comm.* 200, 327–336.

Jayaraman, G. (1983). Water transport in the arterial wall-A theoretical study. *J. Biomechanics.* 16, 833-840.

Kenyon, D. E. (1976). The theory of an incompressible solid-fluid mixture. *Arch. Rat. Mech. Anal.* 62, 131-147.

Mow, V. C., M. K. Kwan, W. M. Lai and M. H. Holmes (1985). A finite deformation theory for non-linearly permeable soft hydrated biological tissues. *Frontiers in Biomechanics, G. Schmid-Schoenbein, S. L. Y. Woo and B. W. Zweifach (eds), Springer-Verlag,* New York. 153-179.

Muskat, M. (1937). Flow of homogeneous fluids through

Noreen Sher Akbar, S. N. and C. Lee (2013). Characteristics of Jeffrey fluid model for peristaltic flow of chime in small intestine with magnetic field. *Results in Physics.* 3, 152–160.

Oomens, C. W., D. H. Van Campen and H. J. Grootenboer (1987). A mixture approach to the mechanics of skin. *J. Biomechanics.* 20, 877-885.

Porous media. McGraw-Hill, New York.

Prasad, K. V., H. Vaidya and K. Vajravelu (2015). MHD Mixed Convection Heat Transfer in a Vertical Channel with Temperature-Dependent Transport Properties. ***J**ournal of **A**pplied **F**luid **M**echanics* 8(4), 693-701.

Rashidi, M. M. and E. Erfani (2012). Analytical method for solving steady MHD convective and slip flow due to a rotating disk with viscous dissipation and ohmic heating. *Engineering Computations* 29(6), 562–579.

Rashidi, M. M. and N. Freidoonimehr (2014). Analysis of Entropy Generation in MHD Stagnation-Point Flow in Porous Media with Heat Transfer. *International Journal for Computational Methods in Engineering Science and Mechanics.* 15, 345–355.

Rashidi, M. M., B. Rostami, N. Freidoonimehr and S. Abbasbandy (2014a). Free Convective Heat and Mass Transfer for MHD Fluid Flow over a Permeable Vertical Stretching Sheet in the Presence of the Radiation and Buoyancy Effects. *Ain Shams Engineering Journal*. 5(3), 901-912.

Rashidi, M. M., E. Momoniat, M. Ferdows and A. Basiriparsa (2014b). Lie group solution for free convective flow of a nanofluid past a chemically reacting horizontal plate in a porous media. *Mathematical Problems in Engineering*, 239082.

Rashidi, M. M., F. Mohammadi, S. Abbasbandy and M. S. Alhuthali (2015). Entropy Generation Analysis for Stagnation Point Flow in a Porous Medium over a Permeable

Stretching Surface. ***J**ournal of **A**pplied **F**luid **M**echanics* 8(4), 753-765.

Rashidi, M. M., S. Abelman and N. Freidooni Mehr (2013b). Entropy generation in steady MHD flow due to a rotating porous disk in a nanofluid. *International Journal of Heat and Mass Transfer*. 62, 515–525.

Rashidi, M. M., T. Hayat, M. Keimanesh and A. A. Hendi (2013a). New Analytical Method for the Study of Natural Convection Flow of a non-Newtonian fluid. *International Journal of Numerical Methods for Heat and Fluid Flow*. 23(3), 436-450.

Rudraiah, N. and S. T. Nagaraj (1977). Natural convection through vertical porous stratum. *Int. J. Engng. Sci.* 15, 589-600.

Santhosh, N. and D. Radhakrishnamacharya (2014). Jeffrey Fluid Flow through Porous Medium in the Presence of Magnetic Field in Narrow Tubes. Hindawi Publishing Corporation. *International Journal of Engineering Mathematics Article*. 1-8.

Shadloo, M. S. and A. Kimiaeifar (2011). Application of homotopy perturbation method to find an analytical solution for magnetohydrodynamic flows of viscoelastic fluids in converging/diverging channels, *Proc. IMechE Part C: J. Mechanical Engineering Science 225*.

Sreenadh, S., M. Krishnamurthy., E. Sudhakara and G. Gopikrishna (2014). Couette flow over a deformable permeable bed. *International Journal of Innovative Research in Science and Engineering*.

Sreenadh, S., P. Madhu Mohan Reddy, E. Sudhakara and A. Parandhama (2013). Free Convective MHD Jeffrey Fluid Flow between Two Coaxial Inclined Permeable Cylinders. *International Journal of Engineering Sciences and Research Technology* 2(11), 3189-3194.

Srinivas, S. and R. Muthuraj (2011). Effects of chemical reaction and space porosity on MHD mixed convective flow in a vertical asymmetric channel with peristalsis. *Mathematical and Computer Modelling* 54(5), 1213–1227.

Terzaghi, K. (1925). Erdbaum echanikauf Grundlagen.

Turner, M. R., G. C. Clough and C. C. Michel (1983). The effects of cationised ferrit in and native ferrit in upon filtration coefficients of single frog capillaries. Evidence that proteins in the endothelial cell coat influence permeability. *Microvascular Res*. 25, 205-222.

Umavathi, J. C. and M. S. Malashetty (1999). Oberbeck convection flow of a couple stress fluid through a vertical porous stratum. *International Journal of Non-Linear Mechanics* 34(6), 1037–1045.

Vajravelu, K., S. Sreenadh and P. Lakshminarayana (2011). The influence of heat transfer on peristaltic transport of a Jeffrey fluid in a vertical porous stratum. *Int Commun Nonlinear SciNumber Simulat*. 16, 3107–3125.

Wen, P. H., Y. C. Hon and W. Wang (2009). Dynamic responses of shear flows over a deformable porous surface layer in a cylindrical tube. *Applied Mathematical Modelling*. 33, 423–436.

Zaheer, A. and T. Hayat (2008). Radiation effects on MHD flow in a porous space. *International Journal of Heat and Mass Transfer*. 51, 1024–1033.

Appendix

$$a_1=\sqrt{\delta\eta},\frac{dp}{dx}=G,a_2=\frac{1-\phi_f G}{a_1^2},a_3=\frac{B_1^2\cosh 2a_1\sqrt{1+\lambda_1}}{1+\lambda_1}+\frac{a_1^2a_2^2}{2}+4a_2\frac{B_1\cosh a_1\sqrt{1+\lambda_1}}{1+\lambda_1},$$

$$a_4=\frac{a_3-\phi_f G}{a_1^2}-\frac{a_2^2}{a_1^2(1+\lambda_1)},a_5=\frac{a_2^2}{2},a_6=\frac{B_1^2}{3a_1^2(1+\lambda_1)},a_7=\frac{2a_2B_1}{a_1\sqrt{1+\lambda_1}}$$

$$a_8=a_5-a_4-a_6\cosh 2a_1\sqrt{1+\lambda_1}-a_7\sinh 2a_1\sqrt{1+\lambda_1},a_9=\frac{\phi_s G-a_4a_1^2}{2},$$

$$a_{10}=\frac{a_5a_1^2}{12},a_{11}=\frac{2a_7}{a_1\sqrt{1+\lambda_1}}-2B_3,\mathrm{a}_{12}=\frac{a_6}{4(1+\lambda)},a_{14}=\frac{\phi_s G-a_1^2a_2}{2},$$

$$a_{15}=a_{12}\cosh 2a_1\sqrt{1+\lambda_1}+a_7\frac{\sinh a_1\sqrt{1+\lambda_1}}{1+\lambda_1}-a_{11}\frac{\cosh a_1\sqrt{1+\lambda_1}}{1+\lambda_1}-a_9-a_{10},$$

$$B_1=\frac{-a_2}{2\cosh a_1\sqrt{1+\lambda_1}},\mathrm{B}_3=\frac{a_8}{2\cosh a_1\sqrt{1+\lambda_1}},C_1=\frac{2B_1\cosh a_1\sqrt{1+\lambda_1}}{1+\lambda_1}-a_{14}$$